A Journal of the Gesellschaft Deutscher Chemiker
Angewandte Chemie
GDCh
International Edition
www.angewandte.org

Accepted Article

Title: High Precision Size Recognition and Separation in Synthetic 1D Nanochannels

Authors: Donglin Jiang, Ping Wang, Qiuhong Jiang, Xinyi Chen, Matthew Addicoat, Ning Huang, Sasanka Dalapati, Thomas Heine, and Fengwei Huo

To be cited as: *Angew. Chem. Int. Ed.* 10.1002/anie.201909851
Angew. Chem. 10.1002/ange.201909851

Link to VoR: http://dx.doi.org/10.1002/anie.201909851
http://dx.doi.org/10.1002/ange.201909851

WILEY-VCH

High Precision Size Recognition and Separation in Synthetic 1D Nanochannels

Ping Wang,[a] Xinyi Chen,[a] [b] Qiuhong Jiang, [a] Matthew Addicoat,[c] Ning Huang,[a] Sasanka Dalapati,[a] Thomas Heine,[d] Fengwei Huo,[b] and Donglin Jiang*[a] [e]

Abstract: Covalent organic frameworks (COFs) allow elaborate manufacture of ordered one-dimensional channels in the crystal. While this makes designing by topology diagram particularly attractive as a tool for assembling straight pores to facilitate mass transport, molecular recognition has been so far inaccessible. We define a superlattice of COFs, by engineering channels with persistent triangular shape and discrete pore size. We observe a size recognition regime that is different from the characteristic adsorption of COFs, where pore window and walls are cooperative so that triangular apertures sort molecules of one-atom difference and notch nanogrooves confine them into single-file molecular chains. The recognition and confinement are accurately described by sensitive spectroscopy and femto-second dynamic simulations. The resulting COFs enable instantaneous separation of mixture to achieve infinite selectivity and 100% purity at ambient temperature and pressure. Our findings offer an approach to merge precise recognition, selective transport, and instantaneous separation in synthetic 1D channels.

Introduction

One-dimensional (1D) nanochannels offer an ideal molecular conduit for mass transport as observed in biological ion channels and synthetic porous materials.[1] Assimilating molecular size recognition regime into 1D channels could create materials with exceptional separation and selective transportation properties. In addition to accurate pore dimension and shape, ion channels enable size recognition by elaborating precise spatial organization of polypeptide segments on the pore wall as a checkpoint to identify ions.[1a] Artificial 1D nanochannels can be prepared using three major methods, including phase-separation driven self-assembly of block copolymers to form nanodomain structure followed by chemical etching to yield cylindrical nanoholes[2], liquid crystal-templated silication to form mesoporous hexagonal silicates[3], and topology-directed polycondensation to produce covalent organic frameworks (COFs) with built-in polygon pores[4]. However, these straight channels usually have uniform chemical compositions on the pore wall, precluding the possibility of manufacturing specific wall sectors to create a checkpoint for size recognition. Thus, engineering synthetic 1D channels to develop size recognition property is a challenge.

COFs elaborate various organic units to generate extended crystalline frameworks via polycondensation in which covalent bond and non-covalent interactions are integrated to direct the covalent growth of two-dimensional (2D) polymer sheets and to control the mode of π stacking, constituting ordered yet dense 1D synthetic nanochannels across the material.[5] Owing to the broad diversity of building units, COFs create 1D channels with different polygon shapes ranging from hexagon to tetragon and trigon. These 1D channels have been developed for adsorption and transport of various molecules.[1a,5] However, how to explore the 1D channels of COFs for size recognition is unprecedented and remained to be well explored.

Here we show for the first time the strategy for developing 1D channels of COFs to recognize molecular size. We observed a size recognition mechanism that is different from the typical adsorption behavior of COFs in which the pore window and walls are cooperative so that the shape persistent triangular apertures can sort molecules of one-atom difference and the notch nanogrooves confine them into single-file molecular chains. Moreover, we scrutinized the structural origins of the size recognition regime in the synthetic 1D channels and demonstrate their exceptional functions in size recognition and separation. We elucidated the structure-function correlation by disclosing the structural parameters that control the size recognition process. We highlighted that the frameworks are capable of combining precise recognition, selective transport and instant separation in one material.

Results and Discussion

We designed and synthesized artificial 1D channels that enable accurate size recognition by topology-directed lattice engineering of COFs (Figure 1, HFPTP-BPDA-COF). We developed a superlattice of 1D channels with persistent triangular shape and discrete pore size. The HFPTP-BPDA-COF was synthesized by topology-guided polycondensation of the C_3-symmetric 2,3,6,7,10,11-hexakis(4-formylphenyl)triphenylene (HFPTP) and the C_2-symmetric 1,1'-biphenyl-4,4'-diamine (BPDA) under solvothermal condition (Figure 1a). Each channel

---

[a] Dr. P. Wang, X. Chen, Dr. Q. Jiang, Dr. N. Huang, Dr. S. Darapati, Prof. Dr. D. Jiang
Department of Chemistry, Faculty of Science, National University of Singapore, 3 Science Drive 3, Singapore 117543, Singapore.
E-mail: chmjd@nus.edu.sg
[b] X. Chen, Prof. Dr. F. Huo
Key Laboratory of Flexible Electronics & Institute of Advanced Materials, Nanjing Tech University, 30 South Puzhu Road, Nanjing 211816, P. R. China.
[c] Dr. M. Addicoat
School of Science and Technology, Nottingham Trent University, Nottingham, NG11 8NS, UK.
[d] Prof. Dr. T. Heine
Department of Theoretical Chemistry, TU Dresden, Mommsenstr. 13, 01062 Dresden, Germany.
[e] Prof. Dr. D. Jiang
Joint School of National University of Singapore and Tianjin University, International Campus of Tianjin University, Binhai New City, Fuzhou 350207, P. R. China.

Supporting information for this article is given via a link at the end of the document.

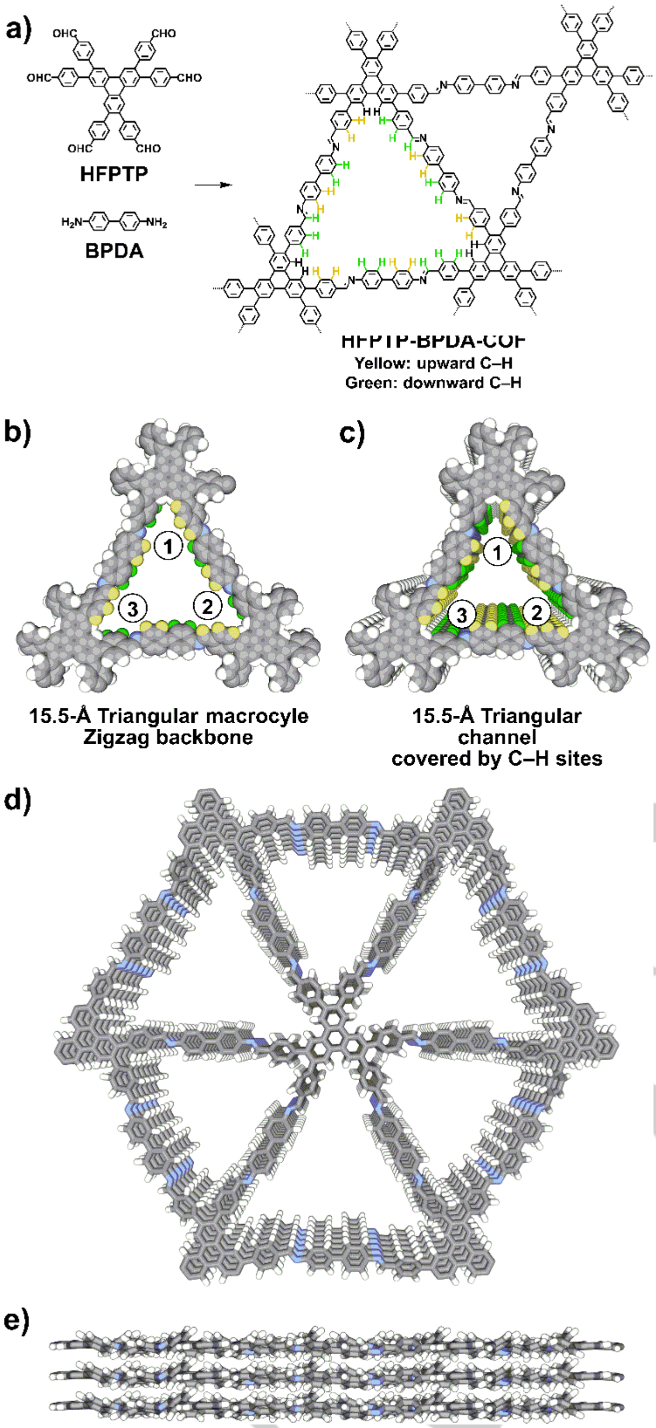

Figure 1 a) Schematic representation of the synthesis of HFPTP-BPDA-COF. Reconstructed crystal structures of b) one triangular macrocycle with zigzag backbones and a 15.5-Å pore size and c) many layers of the 1D 15.5-Å triangular channel coved by sequenced upward and downward C–H sites (yellow for upward C–H and green for downward C–H sites relative to the 2D sheet). Each triangular channel consists of three equivalent V-shaped corner nanogrooves (indicated by ①,②, and ③) with readily accessible C–H sites. Reconstructed crystal structures of d) top and e) side views of the extended dual-pore triangular superlattice.

consists of three V-shaped nanogrooves at three corners (Figure 1b, c) formed by π stacking of triangular macrocycle (Figure 1b); the three equivalent walls are covered by sequenced zigzag C–H units extruded from the backbones (Figure 1c) and readily accessible to guest molecules. The triangular superlattice is covalently fixed by the two-dimensional (2D) sheet (Figure 1d) and further locked by π stacking (Figure 1e). We unexpectedly found that the triangular channels enable size recognition to identify molecules of one-atom difference, thus opening an unprecedented strategy that can integrate precise recognition, selective transport, and instant separation into one channel.

The chemical structure of HFPTP-BPDA-COF was characterized by various analytical methods (see supplementary materials, (Figures. S1-S5, and Tables S1-S3). Fourier transform infrared spectroscopy (Figure S1) revealed a new peak at 1620 cm^{-1} assignable to the imine linkage[6], indicating the polycondensation between HFPTP and BPDA (Figure S2). Solid-state ^{13}C nuclear magnetic resonance spectroscopy (Figure S2) revealed that the peak at 157 parts per million (ppm) is assigned to the C atom of the C=N bond, indicating the formation of imine linkages in HFPTP-BPDA-COF.[6] Thermogravimetric analysis suggested that HFPTP-BPDA-COF was stable up to 500 °C under nitrogen (Figure S3).

The HFPTP-BPDA-COF exhibited powder X-ray diffraction (PXRD) signals at 3.42°, 5.98°, 6.96°, 9.26°, 10.38°, and 24.71°, which were assigned to the (100), (110), (200), (210), (300), and (001) facets, respectively (Figure 2a, red curve). The presence of the (001) facet suggests the structural ordering with 3.64-Å separation in the z direction perpendicular to the 2D layers (Figure 1e). We used density functional based tight binding (DFTB+) calculations[7] to optimize the conformation of the 2D single layer and the configurations of different stacking modes (Table S1). The energetically most favorable slipped AA stacking mode yielded a PXRD pattern (Figure 2a, blue curve) that is in good agreement with the experimentally observed profile. The Pawley refinement using the P1 space group (Figure 2a, green curve) with the unit cell parameters of a = 30.0679 Å, b = 30.0863 Å, c = 7.6352 Å, α = 89.8782°, β = 90.1544°, and γ = 60.0872° reproduced the PXRD pattern with negligible deviations (Figure 2a, black curve). Tables S2 and S3 summarize the atomic coordinates of DFTB+ and Pawley refinement. Thus, the reconstruction reveals an extended dual-pore superlattice with ordered triangular 1D channels (Figure 1d).

The HFPTP-BPDA-COF exhibited reversible nitrogen sorption isotherm curves (Figure 2b) with a Brunauer-Emmett-Teller (BET) surface area of 1024 m^2 g^{-1}. Pore size distribution profile revealed the presence of two different pores with size of 12.7 and 15.5 Å, respectively (Figure 2c). This is consistent with the superlattice structure (Figure 1d).

We probed size recognition of HFPTP-BPDA-COF using electronic absorption spectroscopy. Nile red (NR), 7-(diethylamino)-3-phenylcoumarin (DAPC), and coumarin 6 (C6) (Figure 3a) are similar in the backbone, are bulky to contain more than 40 atoms, and have a difference of one atom between NR

10.1002/anie.201909851

and C6. The big difference in the wavelength of absorption band between NR (523 nm), DAPC (393 nm), and C6 (446 nm) enables a distinct detection of each compound in mixture; their high absorption coefficients (> 36,000 M^{-1}) warrant a quantitative and sensitive monitoring of the recognition process.

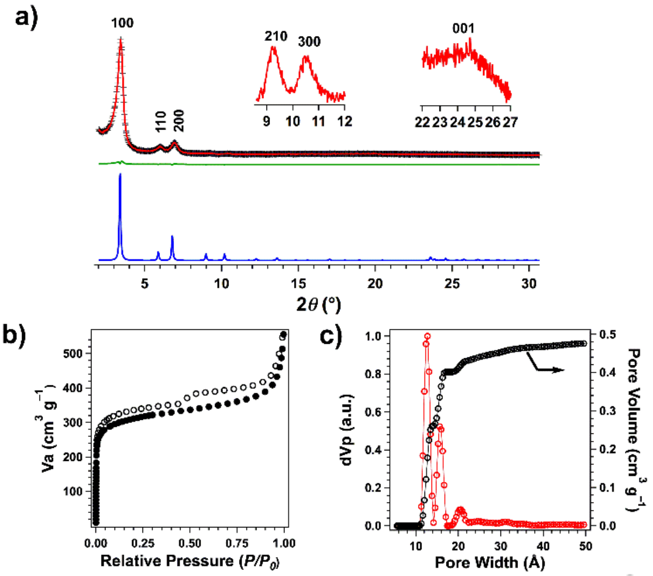

Figure 2 a) PXRD profiles of HFPTP-BPDA-COF of experimentally observed PXRD pattern (red curve), Pawley-refined PXRD pattern (black curve), the difference (green curve) between them, and simulated pattern with the 2.0-Å slipped AA-stacking model (blue curve). The insets are the enlarged PXRD patterns. b) Nitrogen-sorption isotherm curves measured at 77 K (filled circles for sorption and open circles for desorption). c) Profiles of the pore size distribution (red dots) and pore volume distribution (black dots).

We added the HFPTP-BPDA-COF crystallites to a THF solution of NR (15.0 Å in size) and monitored the resulting solution using time-dependent spectroscopy. After only 1 min, a sharp drop of the NR absorbance was observed (Figure 3b), indicating a rapid uptake of NR by HFPTP-BPDA-COF. Notably, HFPTP-BPDA-COF uptakes nearly all NR molecules within 2 min (Figure 3b, red curve; Figure 3e, red circles). In contrast, under otherwise identical conditions, the THF solution of C6 (16.8 Å in size) did not show any spectral change even after 12 h (Figure 3c; Figure 3e, blue triangles). This result suggests that the triangular channels completely reject the entry of C6, which is larger than NR by one atom. More explicitly, DAPC (15.5 Å) that is comparable to the pore aperture (15.5 Å) was also rejected by the channels, without showing any spectral change upon addition of HFPTP-BPDA-COF, irrespective of immersion time (Figure 3d; Figure3e, black circles). These clear differences revealed that the triangular aperture in HFPTP-BPDA-COF serves as a checkpoint to recognise a subtle difference of size and to sort molecules into 1D channels.

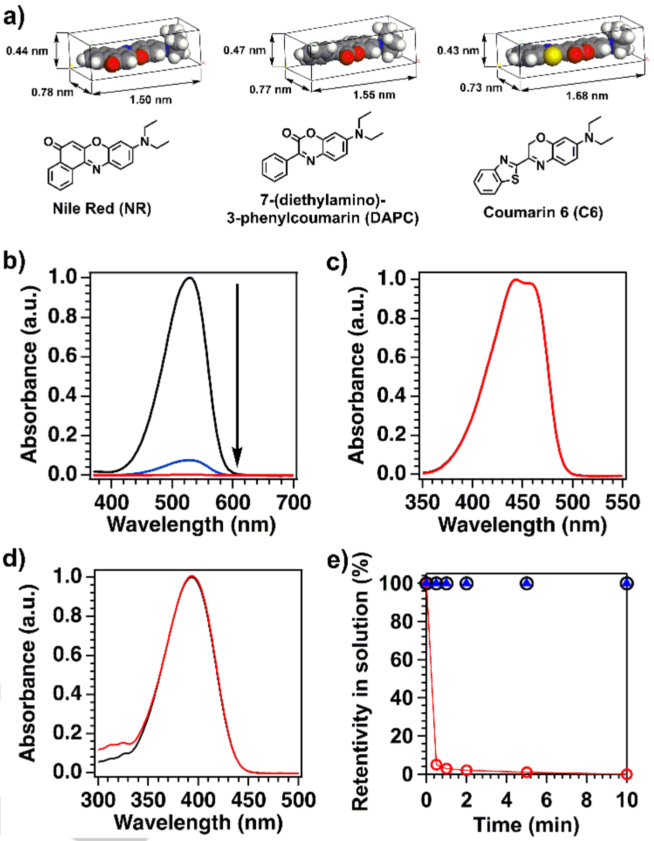

Figure 3 a) Chemical structure and dimension of nile red (NR), 7-(diethylamino)-3-phenylcoumarin (DAPC), and Coumarin 6 (C6). b) Electronic absorption spectral change of the THF solution of NR upon addition of the insoluble HFPTP-BPDA-COF crystallites (black curve, pristine solution; blue curve, 1 min after addition; red curve, 2 min after addition). Electronic absorption spectra of the THF solution of c) C6 and d) DAPC upon addition of HFPTP-BPDA-COF (black curve, pristine solution; red curve, 12 h after addition; overlapped). e) Time-dependent retentivity of NR (red circles and line), C6 (blue triangles), and DAPC (black circles) in the THF solutions after addition of HTP-BDA-COF.

To verify that the uptake occurred in the channels, we investigated the nitrogen sorption isotherms of HFPTP-BPDA-COF after the NR uptake. The resulting COF samples exhibited a sharp decrease in the BET surface area from 1024 to 730 m^2 g^{-1} (Figure S4a). More clearly, pore size distribution profile (Figure S4b) revealed that the 15.5-Å channel almost disappeared. Pore volume profile (Figure S4c) revealed that the 12.7-Å pore did not show any change and the 15.5-Å channels are fully occupied. As a control, HFPTP-BPDA-COF after addition to the DAPC solution did not change the nitrogen sorption profiles as DAPC cannot enter into the pores (Figure S5). Therefore, the 15.5-Å channels account for the recognition and nanoconfinement.

To confirm if the recognition is dependent on the channel shape, we conducted control experiments using tetragonal and hexagonal COFs[6, 8] that have the same pore size as that of HFPTP-BPDA-COF. We observed that neither the tetragonal TTA-TFB-COF (Figure S6, a-e) nor the hexagonal TFBCz-PDA-COF (Figure S6, f-j) caused a change of the absorption spectra

10.1002/anie.201909851

even after 12 h. These results rationalize our strategy that the triangular shape is of fundamental importance for size recognition.

A possible scenario of the process was revealed by molecular dynamic simulations at femto-second level using a global minimum energy protocol.[9] The guest molecules approaching to HFPTP-BPDA-COF take an orientation with their π backbone parallel to the COF π-surface (the (100) facet) whereby the potential energy is minimized (Figure 4a, stage 1). If the guest molecules such as DARP and C6 are larger than the window, the triangular aperture blocks their entry (Figure S7) so that they are left in solution. Once the NR molecules pass the aperture (Figure 4a, stage 2), they rotate in the channels to take a diving pose (Figure 4a, stage 3) with their π backbones parallel to the long axis of channels and are successively confined at the corner nanogrooves (Figure 4a, stage 4) to form single file molecular chains in the channel (Figure 4d). These four processes complete within 10 picoseconds. Each 15.5-Å-sized channel has three nanogrooves and confine three single file molecular chains (Figure 4b, c); an 18-nm long channel can dock 30 NR molecules into 3 single file chains at the nanogrooves (Figure 4d). From the density of the 15.5-Å channels, a cubic HFPTP-BPDA-COF crystallite with a dimension of only 500 × 500 × 500 nm^3 confines as more as 7,500,000 NR molecules (Figure 4d). This exceptional confinement definitely originates from a full accessibility of every channel corner in the crystal. Kinetics experiments (Figure S8) revealed an apparent pseudo-second-order rate constant (k_{obs}) of 13.11 mg g^{-1} min^{-1}, which is more than three orders of magnitude higher than those of the state-of-the-art COFs[6] and amorphous porous polymers[10]. The high k_{obs} value also suggests nearly all the space of the channels is accessible.

We analyzed the binding manner and energy in the V-corner confinement. Each NR molecule receives 9 close C–H···π interactions (< 3.0 Å)[11] with the C–H units as well as attractive London dispersion forces (Figure S9) from both walls. The multipoint interactions over 5 layers of a 1.8-nm-long channel (Figure 4c) gain a binding energy of 41.1 kcal mol^{-1}. We virtually inserted C6 into the channel, which resulted in a binding energy of 40.6 kcal mol^{-1}, a same level as that of NR. This simulation excludes the possibility that C6 could once enter into the channel.

We explored the possibility of size recognition in the NR/C6 and NR/DAPC mixtures. Addition of HFPTP-BPDA-COF to the NR/C6 mixture caused the vanish of the NR absorbance (Figure 5a). After only 2 min, NR is completely sorted into the channels (Figure 5b, red circles) while C6 is left in solution (Figure 5b, black circle). The decrement at 446 nm is associated with a certain absorbance of NR at 446 nm. Indeed, after carefully eliminating the effect of NR according to the Beer-Lambert law, the absorbance of the C6 molecules retained. Clearly, the quickness of NR uptake is not interfered by the existence of the same numbers of C6 molecules. For the NR/DAPC mixture, an instant drop of the NR absorption band (Figure 5c) confirms that the 1D channels sort NR molecules quickly into the pores upon only a short exposure (Figure 5d, red circles) and leave DAPC molecules in the solution phase (Figure 5d, black circles). Thus, the triangular channels can recognize the size difference in mixtures and endow HFPTP-BPDA-COF with a potential of exceptional separation. As COFs are versatile in pore wall engineering[12], our strategy offers an approach to designable 1D channels for precise size recognition, selective transport, and quick separation.

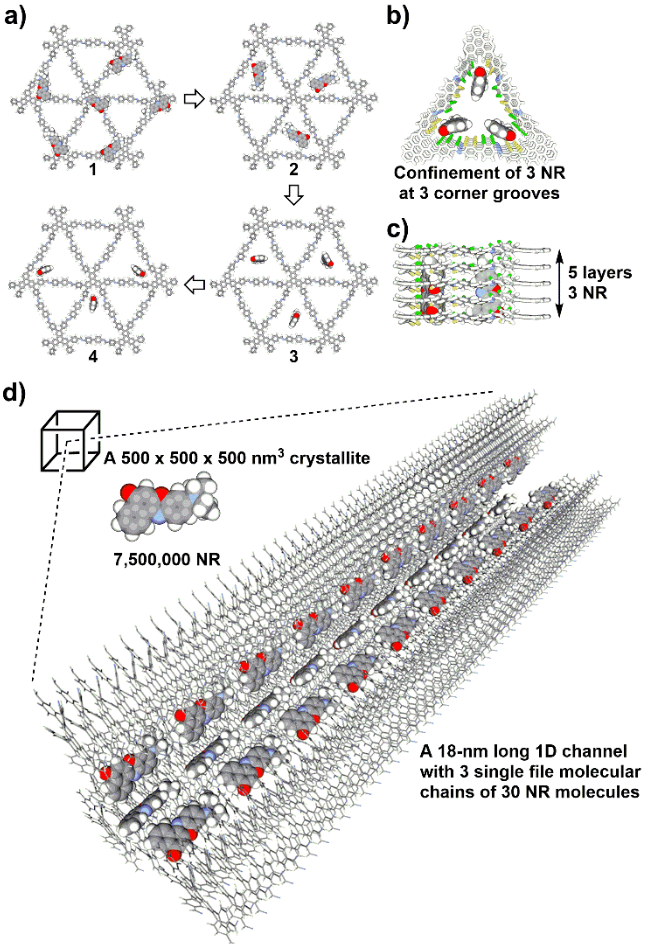

Figure 4 a) The process of size recognition and nanoconfinement by HFPTP-BPDA-COF. The reconstructed structure of b) top and c) side views of 3 NR molecules in a 15.5-Å triangular channel over 5 layers and 1.8-nm length. d) A cubic HFPTP-BPDA-COF crystallite with the dimension of only 500 × 500 × 500 nm^3 confines over 7,500,000 NR molecules. Inset, the reconstructed structure of a triangular channel in 50 layers over 18 nm length for the confinement of 30 NR molecules into 3 single file molecular chains at its nanogrooves.

We demonstrated the separation of the NR/C6 or NR/DAPC mixtures using HFPTP-BPDA-COF columns. A THF solution of NR/C6 (totally 0.02 mmol, 1/1 mol/mol) was subjected to an open column of HFPTP-BPDA-COF (30 mg; 1.5 cm long in column) followed by a THF flow at ambient temperature and pressure. The green-coloured C6 fraction comes out from the column as soon as the THF solvent flows out, enabling a swift separation of C6 from NR. Indeed, the C6 fraction flushed out completely within 2 min to yield 100% purity (Figure 5e, black curve; Figure S10), leading to a separation with infinite selectivity (Figure 5e, blue

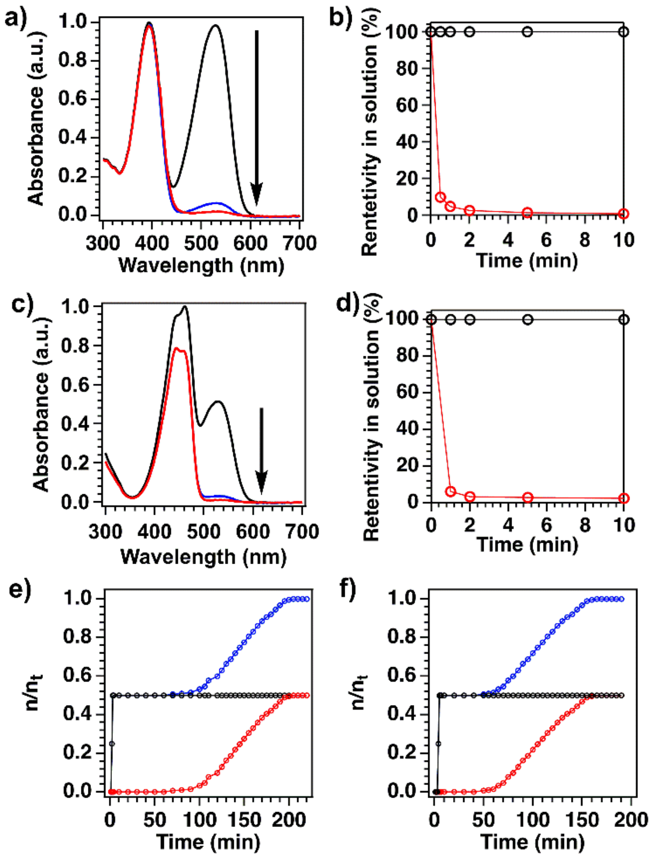

Figure 5 a) Electronic absorption spectral change of the THF solution of a mixture of NR/DAPC (1/1 molar ratio), upon addition of HTP-BDA-COF (black curve, pristine; blue curve, after 30 s; red curve, after 2 min). b) Time-dependent retentivity of NR (red circles and curve) and DAPC (black circles and curve) in solution. NR is sorted into the channels and DAPC is retained in solution. c) Electronic absorption spectral change of the THF solution of a mixture of NR/C6 (1/1 molar ratio), upon addition of HTP-BDA-COF (black curve, pristine; blue curve, after 30 s; red curve, after 2 min). d) Time-dependent retentivity of NR (red circles and curve) and C6 (black circles and curve) in solution. NR is sorted into the channels and C6 is retained in solution. e) The COF column flow-out charts of C6 (black curve), NR (red curve), and C6 plus NR (blue curve) for a mixture of NR/C6 at 1/1 molar ratio at ambient temperature and pressure. f) The COF column flow-out charts of DAPC (black curve), NR (red curve), and DAPC plus NR (blue curve) for a mixture of NR/DAPC at 1/1 molar ratio at ambient temperature and pressure.

curve). The NR fraction was also pure and came out in 70-200 min as the NR molecules were sorted into the channels (Figure 5e, red curve). In the same way, the HFPTP-BPDA-COF column separates the NR/DAPC mixture (Figure 5f, blue curve) into DAPC within 2 min (Figure 5f, black curve; Figure S11) and NR in 60-160 min (Figure 5f, red curve). These results also suggest that the triangular channels enable quick uptake but slow release; this character is helpful for a molecular delivery system to achieve a constant release.[13] Notably, the COF columns upon five cycles retain their functions (Figure S12) as well as crystallinity and porosity Supplementary Figure S13 and S14). Finally, we used the commercial silica gel (700 mg; 23-fold that of the COF weight; 7-cm long column; THF) to separate the mixtures by their polarity difference in THF and observed that they cannot be separated (Figure S15). Thus, the recognition and separation as well as transportation by the 1D channels are not based on polarity but driven solely by a subtle difference of molecular size.

Conclusion

In summary, we have established a strategy for size recognition of synthetic 1D nanochannels, by exploring a latticed framework with shape-persistent triangular pores. One important knowledge we disclosed through this study is that the 2D π surface of the framework, the triangular aperture and the pore walls with built-in C–H sequences are key structural parameters in size recognition. Their cooperativeness renders the COF able to combine precise size recognition of one atom difference, selective docking and transport and instant separation in one material, demonstrating the strength of 1D channels for accurate molecular recognition and separation – an ultimate goal of porous materials in implementation. These unique properties of synthetic 1D channels are established for the first time in COFs and would exert great impact on the further advance of the field. We envisage that synthetic 1D channels could offer a promising platform for designing robust size recognition devices that are useful in adsorption, transportation and separation.

Acknowledgements

D.J. acknowledges MOE tier 1 grant (R-143-000-A71-114). M.A. acknowledges support from EPSRC, EP/S015868/1 and HPC resources on T.H. via the Materials Chemistry Consortium, EP/P020194. T.H. acknowledges financial support via Deutsche Forschungsgemeinschaft, SPP 1928 COORNETs, under contract number HE 3543/30-1.

Keywords: covalent organic framework• size recognition • separation • 1D nanochannels • trigonal topology

[1] D. A. Doyle, J. M. Cabral, R. A. Pfuetzner, A. Kuo, J. M. Gulbis, S. L. Cohen, B. T. Chait, R. MacKinnon, *Science* **1998**, *280*, 69-77. b) N. Huang, P. Wang, D. Jiang, *Nat. Rev. Mater.* **2016**, *1*, 16068. doi: 10.1038/natrevmat2016.68.

[2] V. Abetz, P. F. W. Simon in *Polymer Science, vol. 189.* (Eds.: V. Abetz), Springer, Berlin, Heidelberg, **2005**, pp.125-212.

[3] C. T. Kresge, M. E. Leonowicz, W. J. Roth, J. C. Vartuli, J. S. Beck, *Nature* **1992**, *359*, 710-712.

[4] a) P. J. Waller, F. Gándara, O. M. Yaghi, *Acc. Chem. Res.* **2015**, *48*, 3053-3063. b) J. W. Colson, A. R. Woll, A. Mukherjee, M. P. Levendorf, E. L. Spitler, V. B. Shields, M. G. Spencer, J. Park, W. R. Dichtel, *Science* **2011**, *332*, 228-231. c) J. Guo, et al., *Nat. Commun.* **2013**, *4*, 2736. doi: 10.1038/ncomms3736.

[5] a) T. Ma, et al., *Science* **2018**, *361*, 48-52. b) X. Guan, H. Li, Y. Ma, M. Xue, Q. Fang, Y. Yan, V. Valtchev, S. Qiu, *Nat. Chem.* **2019**, *11*, 587-594. c) L. Ascherl, et al., *Nat. Chem.* **2016**, *8*, 310-316. d) S. Kandambeth, A. Mallick, B. Lukose, M. V. Mane, T. Heine, R. Banerjee, *J. Am. Chem. Soc.* **2012**, *134*, 19524-19527. e) M. R. Rao, Y. Fang, S. De Feyter, D. F. Perepichka, *J. Am. Chem. Soc.* **2017**, *139*, 2421-2427. f) R.-B. Lin, B. Chen, *Joule* **2018**, *2*, 1030-1032. g) E. Jin, J. Li, K. Geng, Q. Jiang, H.

Xu, Q. Xu, D. Jiang, *Nat. Commun.* **2018**, *9*, 4143. doi: 10.1038/s41467-018-06719-8. h) L. Zou, X. Yang, S. Yuan, H.-C. Zhou, *CrystEngComm.* **2017**, *19*, 4868-4871.

[6] P. Wang, Q. Xu, Z. Li, W. Jiang, Q. Jiang, D. Jiang, *Adv. Mater.* **2018**, *30*, 1801991. doi: 10.1002/adma.201801991.

[7] a) B. Aradi, B. Hourahine, T. Frauenheim, *J. Phys. Chem. A* **2007**, *111*, 5678-5684. b) http://www.dftb.org

[8] S. Feng, H. Xu, C. Zhang, Y. Chen, J. Zeng, D. Jiang, J.-X. Jiang, *Chem. Comm.* **2017**, *53*, 11334-11337.

[9] M. A. Addicoat, S. Fukuoka, A. J. Page, S. Irle, *J. Comput. Chem.* **2013**, *34*, 2591-2600.

[10] G. Das, T. Skorjanc, T. Prakasam, S. Nuryyeva, J.-C. Olsen, A. Trabolsi, *RSC Adv.* **2017**, *7*, 3594-3598.

[11] M. Nishio, Y. Umezawa, M. Hirota, Y. Takeuchi, *Tetrahedron* **1995**, *51*, 8665-8701.

[12] a) A. Nagai, Z. Guo, X. Feng, S. Jin, X. Chen, X. Ding, D. Jiang, *Nat. Commun.* **2011**, *2*, 536. doi: 10.1038/ncomms1542. b) N. Huang, R. Krishna, D. Jiang, *J. Am. Chem. Soc.* **2015**, *137*, 7079-7082.

[13] K. Park, *J. Controlled Release* **2014**, *190*, 3-8.

Entry for the Table of Contents (Please choose one layout)

Layout 1:

RESEARCH ARTICLE

Open 1D channels enable to recognize molecular size upon designing the pores into triangular shape with discrete pore size in covalent organic frameworks. This finding brings new possibility of 1D channels for selective transport and instant molecular separation with infinite selectivity and 100% purity.

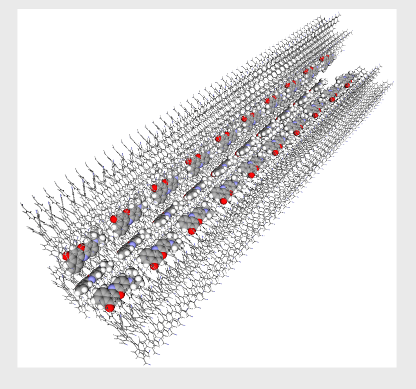

*Ping Wang, Xinyi Chen, Qiuhong Jiang, Matthew Addicoat, Ning Huang, Sasanka Dalapati, Thomas Heine, Fengwei Huo, and Donglin Jiang**

Page No. – Page No.

High Precision Size Recognition and Separation in Synthetic 1D Nanochannels